

## **Observation of the orientation of membrane protein crystals grown in high magnetic force fields**

Nobutaka Numoto<sup>a,1</sup>, Ken-ichi Shimizu<sup>b</sup>, Kazuya Matsumoto<sup>b</sup>, Kunio Miki<sup>b</sup>, Akiko Kita<sup>a,\*</sup>

<sup>a</sup>Research Reactor Institute, Kyoto University, Kumatori, Sennan, Osaka 590-0494, Japan

<sup>b</sup>Department of Chemistry, Graduate School of Science, Kyoto University, Sakyo-ku, Kyoto 606-8502, Japan

<sup>1</sup>Present address: Medical Research Institute, Tokyo Medical and Dental University, 1-5-45 Yushima Bunkyo-ku, Tokyo 113-8510, Japan

\*Corresponding author. Address: Research Reactor Institute, Kyoto University, Kumatori, Sennan, Osaka 590-0494, Japan

Tel: +81-72-451-2379. Fax: +81-72-451-2635

E-mail: [kita@rri.kyoto-u.ac.jp](mailto:kita@rri.kyoto-u.ac.jp)

## **Summary**

Crystallization of membrane proteins in magnetic fields is thought to reveal the magnetic orientations of crystals, and is expected to enhance crystal quality for X-ray crystallographic analysis. The light-harvesting complex 2 (LH2) from a photosynthetic bacterium, *Thermochromatium tepidum* was crystallized in steep-gradient magnetic fields. The rod-shaped crystals of LH2 grown in the magnetic fields were oriented parallel to the magnetic field direction. An X-ray diffraction experiment indicated that the overall  $R$  value and crystal mosaicity are improved for the magnetically oriented crystal, and the helix bundles of LH2 were located parallel to the magnetic field direction in the crystal packing.

## **Highlights:**

The magnetic orientation of the crystals of a membrane protein was observed.

The overall  $R$  value and crystal mosaicity of the oriented crystals were improved.

The helix axis of the molecule was parallel to the magnetic field direction.

## **Keywords:**

A1. Magnetic fields

B1. Biological macromolecules

B3. Superconducting magnet

## 1. Introduction

The production of high-quality single crystals is still one of the most significant hurdles to determining a high-resolution protein structure. Therefore, protein crystallographers have made continuous efforts to grow well-ordered crystals by using all available means of controlling biological, chemical, and physical factors such as protein purity, redox states, and microgravity in space. Crystallization in high magnetic fields is thought to be an effective method of enhancing crystal quality, as reviewed by Sasaki [1]. The most remarkable observation of crystallization under high magnetic fields is that the certain crystallographic axis of the crystals was aligned parallel to the magnetic field direction [2,3,4,5]. In many cases, the resolution limit, mosaicity, overall B-factor, and other aspects of the quality of oriented crystals have been improved [6,7]. The orientation of crystals occurs in both static and gradient magnetic fields. In gradient magnetic fields, diamagnetic waters and protein molecules receive a magnetic force and the upward magnetic force can suppress the natural convection due to gravity [8]. Therefore, crystallization under the gradient magnetic fields (magnetic force fields) provides additional favorable effects for protein crystals because the relatively slow supply rate of protein molecules could improve quality by decreasing the undesired impurity uptake during crystal growth [8,9].

The mechanism underlying the magnetic orientation of protein crystals has not yet been fully understood. The diamagnetic anisotropy of a protein molecule due to the contribution of the planar peptide bonds and aromatic residues has been proposed [10]. In an  $\alpha$ -helix structure, the peptide bond planes form an axial arrangement, hence all the peptide bond planes are oriented parallel to the helix axis. In a  $\beta$ -sheet structure, the peptide bond planes are also oriented almost parallel to the pleat structure. Therefore,

both of the secondary structures of a protein molecule exhibit some diamagnetic anisotropy. It has been suggested that, if most of the secondary structures are arranged in a specific direction in a molecule, the crystal should be oriented parallel to the magnetic field. Membrane proteins are one of the most challenging targets for crystallization because of their amphipathic nature. On the other hand, most membrane proteins possess well-oriented  $\alpha$ -helices or  $\beta$ -strands of a  $\beta$ -barrel structure in the transmembrane region. Thus, membrane proteins are expected to exhibit large diamagnetic anisotropy, and crystallization in magnetic fields is expected to provide an advantage for enhancing crystal quality when molecular arrangement is tandemly aligned [1].

In this paper, we report the first observation of the magnetic orientation of the crystals of a membrane protein, the light-harvesting complex 2 (LH2), from a thermophilic photosynthetic bacterium, *Thermochromatium tepidum*. LH2 is composed of transmembrane  $\alpha$ -helices [11], which are thought to form a ring structure aligned perpendicular to the membrane, because the crystal structures of the bacterial LH2 homologues reveal 8- or 9-fold ring structures [12,13]. This completely aligned  $\alpha$ -helical structure is an ideal model for evaluation of the effects of high magnetic force fields or high magnetic fields on crystallization of membrane protein molecules. X-ray diffraction experiments indicated that the helix axes in the crystals were aligned parallel to the magnetic field direction. The crystal qualities were evaluated both for crystals obtained in high magnetic force fields and those obtained under a control condition.

## **2. Materials and Methods**

### **2.1. Purification**

*T. tepidum* was grown under luminescent conditions according to published procedures [14]. The cells were disrupted by sonication, and the intracytoplasmic membranes of *T. tepidum* were harvested and resuspended in 20 mM Tris-HCl pH 7.5, 500 mM CaCl<sub>2</sub>. The debris were removed by centrifugation, and 10% *n*-Dodecyl- $\beta$ -D-maltopyranoside (DDM) was added to the supernatant (final concentration of 1%). LH2 was solubilized from the membranes by gentle stirring at 4°C overnight. The solution containing the solubilized LH2 was filtered using Vivaspin 500 centrifugal concentrator 300,000 MWCO (Sartorius). The flow-through fraction was concentrated and loaded to a HiLoad 16/60 Superdex 200 column (GE Healthcare) equilibrated with 20 mM Tris-HCl pH 7.5, 50 mM CaCl<sub>2</sub>, 0.05% DDM. Purified protein was desalted with 20 mM Tris-HCl pH 7.5, 0.05% DDM. Preparation of the protein solubilized in *n*-Decyl- $\beta$ -D-maltopyranoside (DM) was performed as follows. LH2 was solubilized from the membranes in the buffer solution containing 20 mM Tris-HCl pH 8.5, 0.05% lauryldimethylamine oxide (LDAO). The solubilized LH2 was loaded to a Mono Q HR10/10 column (GE Healthcare) equilibrated with 20 mM Tris-HCl pH 7.5, 0.05% DM. LH2 was eluted with a linear gradient of 0-1 M NaCl. Purified protein was desalted with 20 mM Tris-HCl pH 7.5, 0.05% DM. For both the DDM and DM-solubilized samples, the protein concentration were adjusted by measuring the absorbance at 853 nm to 100.

### **2.2. Crystallization**

An environment having both a high magnetic field and a steep field gradient was

achieved using a superconducting magnet, JMTA-16T50MF, developed by Japan Superconductor Technology (JASTEC). The superconducting magnet generates a maximum magnetic field of 16.3 T with a  $B_z(dB_z/dz)$  of  $-1540 \text{ T}^2/\text{m}$ , where the direction of the magnetic field is upward. Crystallization experiments were performed in parallel inside and outside the magnetic force fields under the same conditions for 4 weeks. Crystals were obtained by the sitting-drop vapor-diffusion method at 20°C using equal volumes of a protein solution and a reservoir solution containing 13-24% (w/v) polyethylene glycol monomethyl ether (PEG MME) 550, 100 mM MES-NaOH (pH 6.4), and 10 mM zinc sulfate.

### ***2.3. Data collection***

Prior to data collection, the crystals were transferred to the solution, with the concentration increasing stepwise to a final concentration of 30% (v/v) of PEG MME 550. The crystals were then flash-frozen under a nitrogen gas stream at  $-183 \text{ }^\circ\text{C}$ .

X-ray diffraction experiments were performed at Beamlines BL41XU, SPring-8, and BL-1A, KEK-PF. The data were processed and scaled using the HKL2000 package [15] and truncated by the CCP4 program suite [16]. Self-rotation functions were calculated using MOLREP [17]. The statistics for data collection are summarized in Table 1.

### 3. Results and Discussion

LH2 crystals were obtained with precipitant (PEG MME 550) concentrations of 15-23% in the magnetic force fields, and 14-23% in the control (outside of the magnetic force fields) experiment within 4 weeks. The crystals obtained under either condition were rod-shaped and typically  $0.1 \text{ mm} \times 0.1 \text{ mm} \times 0.4 \text{ mm}$ . Almost all of the crystals grown in the magnetic condition were oriented nearly perpendicular in the crystallization drop; the longest edge of the crystals was aligned parallel to the magnetic field direction (Figure 1a, b). No significant differences were observed between the crystals obtained under the magnetic condition and those obtained under the control condition in the maximum crystal sizes, the precipitant concentrations, or the length of time before the crystals appeared. On the other hand, the number of platelike crystals, which were obtained under the conditions of higher precipitant concentrations, were reduced under the magnetic condition (Figure 1c, d). A reduction in the number of crystal nuclei and a relatively slow crystal growth rate were observed in crystallization with static or gradient magnetic fields, as was a magnetic orientation of the crystals [5,9,18]. The observations of our crystallization experiment suggest that the crystal orientation, which is probably due to the magnetic fields, is the major effect on the crystallization of LH2. An additional, minor effect is the suppression of the nuclei of the platelike crystals, which is probably due to the reduced convection by the magnetic force from the gradient magnetic fields.

X-ray diffraction data were collected from crystals obtained in both the magnetic and control conditions (Table 1). We used the crystals from different lots of purified LH2 using DDM (magnet I and control I) or DM (magnet II, III, control II, and III) as a detergent. The maximum resolution of  $7.8 \text{ \AA}$  were obtained both the crystals from the

magnetic and control conditions. However, all the crystals obtained under the magnetic condition show lower overall  $R$  values and mosaicity ranges, except the mosaicity range of the crystal of control II, which show slight a lower range than that of the magnet III, whereas the crystal of control II show worst overall  $R$  value. These facts indicate that the differences of the overall  $R$  value and mosaicity range are statistically significant. In addition, the lower mosaicity ranges of the crystals of the magnetic condition are reproduced despite the different lots of the protein samples and crystallization experiments. These facts confirm that the freezing processes did not affect the mosaicity or the crystal quality. Thus the quality of the LH2 crystals obtained in the magnetic force fields, especially for the magnetically oriented crystals, could be improved. It has been proposed that magnetic orientation occurs when the protein molecules have been organized to a microcrystal, because the magnetic susceptibility of a protein molecule is too small to overcome the thermal energy in a solution [19]. The magnetic orientation of the microcrystals is thought to help reduce the mosaicity of crystals [1]. Because the  $\alpha$ -helical ring structure of LH2 offers the possibilities of an advantage for the diamagnetic anisotropy of the microcrystal, the improvement in the mosaicity of magnetically oriented crystals may have become marked, and thus may have resulted in the improvement in the overall  $R$  value.

The resolution in this study is not yet high enough to determine the molecular structure, but it is sufficient to estimate the orientation of LH2 molecules in the crystal. A self-rotation function of the LH2 crystal indicated that there is a lot of noncrystallographic twofold symmetry in the all-around  $a^*c^*$  plane perpendicular to the crystal  $b$  axis (Figure 2). In addition, noncrystallographic 3- and 4-fold symmetries are observed almost parallel to the crystal  $b$  axis. These observations strongly indicate



that LH2 forms a ring structure composed of aligned transmembrane  $\alpha$ -helices as the crystal structures of the LH2 homologues [12,13], and that the helix axes of LH2 were oriented parallel to the crystal  $b$  axis in the crystal. The orientation of the mounted crystal in the diffraction experiment and the patterns of diffraction spots together confirmed that the crystal  $b$  axis is parallel to the longest edge of the crystal, which was aligned parallel to the magnetic field direction. Thus, we concluded that the helix axes of LH2 were parallel to the magnetic field direction in the crystals of the magnetic condition. This is the first observation of a magnetic orientation of the membrane protein crystals as well as of an aligned helix-rich structure that is indeed oriented parallel to the magnetic field direction. Most membrane proteins possess a helix bundle or a  $\beta$ -barrel structure; both of these are thought to exhibit large diamagnetic anisotropy in the transmembrane region. Our findings strongly suggest that, in most cases, crystals of a membrane protein could be oriented in the magnetic field, and that the oriented crystals could exhibit an enhanced crystal quality if the molecular arrangement in a unit cell is a favorable environment for the diamagnetic anisotropy.

### **Acknowledgments**

The authors thank Prof. Yukio Morimoto for his support. *T. tepidum* was the kind gift of Prof. Zheng-Yu Wang at Ibaraki University. We thank Dr. Kazuki Takeda, Dr. Yu Hirano, and Mr. Masahito Hibi for protein preparations. We also thank the beamline scientists of SPring-8 and KEK-PF where the synchrotron radiation experiments were performed. This work was partly supported by the System Development Program for Advanced Measurement and Analysis (Program-S) from the

Japan Science and Technology Agency (JST).

## References

- [1] G. Sazaki, *Prog. Biophys. Mol. Biol.* 101 (2009) 45.
- [2] J.P. Astier, S. Veessler, R. Boistelle, *Acta Cryst. D* 54 (1998) 703.
- [3] M. Ataka, E. Katohb, N.I. Wakayama, *J. Cryst. Growth* 173 (1997) 592.
- [4] S. Sakurazawa, T. Kubota, M. Ataka, *J. Cryst. Growth* 196 (1999) 325.
- [5] G. Sazaki, E. Yoshida, H. Komatsu, T. Nakada, S. Miyashita, K. Watanabe, *J. Cryst. Growth* 173 (1997) 231.
- [6] S.X. Lin, M. Zhou, A. Azzi, G.J. Xu, N.I. Wakayama, M. Ataka, *Biochem. Biophys. Res. Commun.* 275 (2000) 274.
- [7] T. Sato, Y. Yamada, S. Saijo, T. Hori, R. Hirose, N. Tanaka, G. Sazaki, K. Nakajima, N. Igarashi, M. Tanaka, Y. Matsuura, *Acta Cryst. D* 56 (2000) 1079.
- [8] N.I. Wakayama, *Cryst. Growth Des.* 3 (2003) 17.
- [9] A. Nakamura, J. Ohtsuka, K.-i. Miyazono, A. Yamamura, K. Kubota, R. Hirose, N. Hirota, M. Ataka, Y. Sawano, M. Tanokura, *Cryst. Growth Des.* 12 (2012) 1141.
- [10] D.L. Worcester, *Proc. Natl. Acad. Sci. USA* 75 (1978) 5475.
- [11] F. Sekine, K. Horiguchi, Y. Kashino, Y. Shimizu, L.J. Yu, M. Kobayashi, Z.Y. Wang, *Photosynth. Res.* 111 (2012) 9.
- [12] J. Koepke, X. Hu, C. Muenke, K. Schulten, H. Michel, *Structure* 4 (1996) 581.
- [13] G. McDermott, S.M. Prince, A.A. Freer, A.M. Hawthornthwaitelawless, M.Z. Papiz, R.J. Cogdell, N.W. Isaacs, *Nature* 374 (1995) 517.
- [14] M.T. Madigan, *Int. J. Syst. Bacteriol.* 36 (1986) 222.
- [15] Z. Otwinowski, W. Minor, *Methods Enzymol.* 276 (1997) 307.
- [16] Collaborative Computational Project, Number 4, *Acta Cryst. D* 50 (1994) 760.
- [17] A. Vagin, A. Teplyakov, *J. Appl. Crystallogr.* 30 (1997) 1022.
- [18] S.I. Yanagiya, G. Sazaki, S.D. Durbin, S. Miyashita, K. Nakajima, H. Komatsu, K. Watanabe, M. Motokawa, *J. Cryst. Growth* 208 (2000) 645.
- [19] S.I. Yanagiya, G. Sazaki, S.D. Durbin, S. Miyashita, T. Nakada, H. Komatsu, K. Watanabe, M. Motokawa, *J. Cryst. Growth* 196 (1999) 319.

## Figure Legends

**Figure 1.** LH2 crystals obtained in the high magnetic force fields (a, c) and in the control condition (b, d). Scale bar is shown by the yellow line as 0.2 mm length. The direction of the magnetic fields is perpendicular to the paper.

**Figure 2.** Plots of the self-rotation function for the peaks in the (a)  $\kappa = 180^\circ$ , (b)  $\kappa = 120^\circ$ , and (c)  $\kappa = 90^\circ$  sections. The resolution range and integration radius were 50-8.0 and 53.5 Å, respectively. The two identical peaks in panels (b) and (c) indicate that two molecules of LH2 are contained in the asymmetric unit. (d) The LH2 crystal mounted on the goniometer. (e) A cartoon model of the LH2 molecule. The cylinders represent the transmembrane  $\alpha$ -helices of LH2. The directions of the crystallographic  $b$  axis and magnetic field ( $B$ ) are shown as arrows.

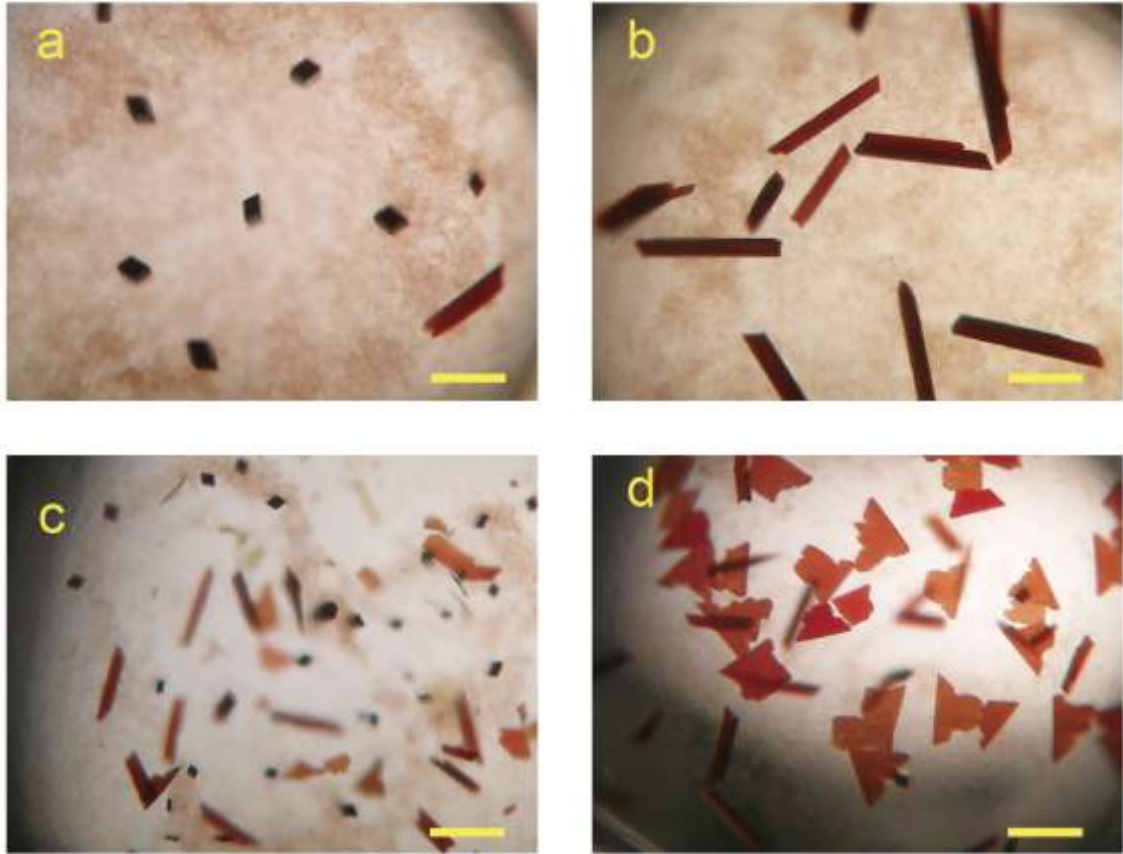


Figure 1. Numoto *et al.*

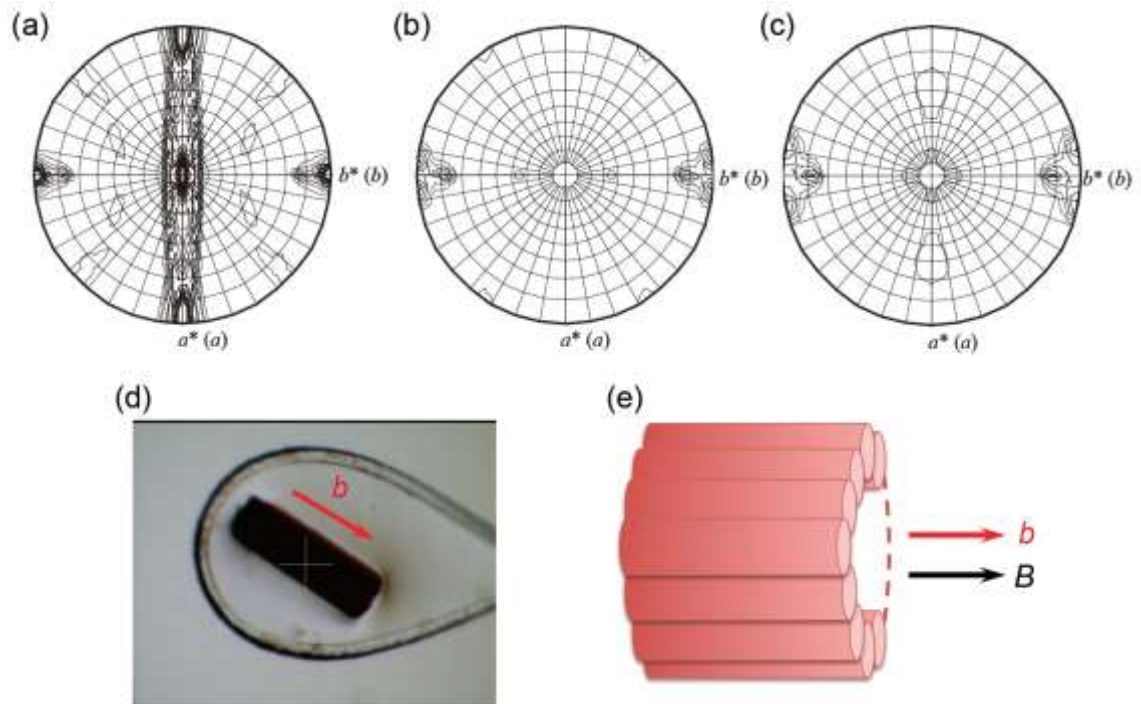


Figure 2. Numoto *et al.*

**Table 1.** Data collection statistics

Data collection	magnet I	magnet II	magnet III	control I	control II	control III
Detergent	DDM	DM	DM	DDM	DM	DM
Wavelength, Å	1.0000	1.1000	1.1000	1.0000	1.1000	1.1000
Space group	$P2_12_12_1$	$P2_12_12_1$	$P2_12_12_1$	$P2_12_12_1$	$P2_12_12_1$	$P2_12_12_1$
Unit-cell parameters, Å						
<i>a</i>	108.8	105.2	104.9	111.2	104.8	104.1
<i>b</i>	117.3	119.6	119.9	115.8	119.3	118.0
<i>c</i>	158.5	156.0	156.1	156.3	156.2	154.4
Resolution, Å	50-7.80	50-7.80	50-7.80	50-7.80	50-7.90	50-9.00
	(8.08-7.80)	(8.08-7.80)	(8.08-7.80)	(8.08-7.80)	(8.18-7.90)	(9.32-9.00)
No. of observations	17,091	14,240	14,459	16,893	12,945	6,055
No. of unique reflections	2,510	2,397	2,422	2,497	2,360	1,561
Completeness, %	99.2 (100)	99.3 (99.6)	99.5 (100)	99.4 (100)	98.9 (100)	96.1 (96.9)
Average $I/\sigma(I)$	37.1 (1.3)	37.3 (1.9)	34.2 (1.5)	35.4 (1.8)	28.4 (1.2)	27.9 (1.4)
Redundancy	6.8 (7.1)	5.9 (6.6)	6.0 (6.6)	6.8 (7.1)	5.5 (6.0)	3.9 (4.2)
Mosaicity range	1.0-1.6	0.97-2.2	1.4-2.2	1.5-2.1	1.2-2.1	1.7-4.1
$R_{\text{sym}}^*$ , %	4.9 (>100)	4.7 (92.6)	5.0 (>100)	5.6 (>100)	8.1 (>100)	6.3 (87.4)

Values in parentheses are for the highest-resolution shell.

\* $R_{\text{sym}} = \frac{\sum \sum_i |I(h) - I(h)_i|}{\sum \sum_i I(h)}$ , where  $I(h)$  is the mean intensity after rejection.